Journal of Nuclear Materials 386–388 (2009) 1–7

Contents lists available at ScienceDirect

Journal of Nuclear Materials

journal homepage: www.elsevier.com/locate/jnucmat

The EU programme for modelling radiation effects in fusion reactor materials: An overview of recent advances and future goals

S.L. Dudarev [a,*], J.-L. Boutard [b,*], R. Lässer [b], M.J. Caturla [c], P.M. Derlet [d], M. Fivel [e], C.-C. Fu [f], M.Y. Lavrentiev [a], L. Malerba [g], M. Mrovec [h], D. Nguyen-Manh [a], K. Nordlund [i], M. Perlado [j], R. Schäublin [k], H. Van Swygenhoven [d], D. Terentyev [g], J. Wallenius [l], D. Weygand [m], F. Willaime [f]

[a] EURATOM/UKAEA Fusion Association, Culham Science Centre, Oxfordshire, OX14 3DB, UK
[b] EFDA Close Support Unit, Boltzmannstrasse 2, D-85748 Garching, Germany
[c] Universitat d'Alacant, Spain
[d] Paul Scherrer Institute, Materials Science and Simulation, Switzerland
[e] Institut National Polytechnique de Grenoble, France
[f] CEA/Saclay, Service de Recherches de Métallurgie Physique, France
[g] SCK-CEN, Mol, Belgium
[h] Fraunhofer-Institut für Werkstoffmechanik, Freiburg, Germany
[i] University of Helsinki, Finland
[j] Universidad Politécnica de Madrid, Spain
[k] Centre de Recherche en Physique des Plasmas, Switzerland
[l] KTH, Sweden
[m] Universität Karlsruhe, IZBS, Germany

A B S T R A C T

The EU fusion materials modelling programme was initiated in 2002 with the objective of developing a comprehensive set of computer modelling techniques and approaches, aimed at rationalising the extensive available experimental information on properties of irradiated fusion materials, developing capabilities for predicting the behaviour of materials under conditions not yet accessible to experimental tests, assessing results of tests involving high dose rates, and extrapolating these results to the fusion-relevant conditions. The programme presently gives emphasis to modelling a single class of materials, which are ferritic-martensitic EUROFER-type steels, and focuses on the investigation of key physical phenomena and interpretation of experimental observations. The objective of the programme is the development of computational capabilities for predicting changes in mechanical properties, hardening and embrittlement, as well as changes in the microstructure and phase stability of EUROFER and FeCr model alloys occurring under fusion reactor relevant irradiation conditions.

1. Introduction

In the paper entitled "The Unreasonable Effectiveness of Mathematics in the Natural Sciences" Wigner [1] noted the potential benefits of applying predictive mathematical models to various problems in natural sciences, technology and engineering. This idea has now taken firm hold in the field of fusion materials, where it is practically difficult, if not impossible, to test the entire range of candidate materials proposed for use in future fusion technology, and to investigate the variety of radiation and thermal conditions expected in a future fusion power plant. Partially the problem comes from the lack of a suitable source of high-energy (~14 MeV) D–T fusion neutrons needed for mimicking the irradiation conditions of a fusion power plant in an experimental test. This issue is expected to be addressed by the future IFMIF facility, which is an accelerator-driven high flux source of 14 MeV neutrons [2]. Another, equally significant, aspect of the fusion materials development comes from the need to extrapolate the results of existing, as well as future IFMIF-based, experimental tests to the more complex and diverse range of conditions expected in a fusion power plant. For example, fission neutron and ion irradiations have shown that the high rates of helium production and atom displacements expected in fusion power plant materials induce significant hardening of ferritic-martensitic steels caused by the high density of helium and vacancy clusters [3,4] as well as by the development of phase instabilities in the FeCr system [5]. Additional embrittlement is expected to result from helium segregation at grain boundaries at low temperatures [4].

* Corresponding authors. Tel.: +44 0 1235 466513 (S.L. Dudarev), +49 89 32 99 43 18 (J.-L. Boutard).
E-mail addresses: Sergei.Dudarev@ukaea.org.uk (S.L. Dudarev), Jean-Louis.Boutard@efda.org (J.-L. Boutard).

0022-3115/$ - see front matter Crown Copyright © 2009 Published by Elsevier B.V. All rights reserved.
doi:10.1016/j.jnucmat.2008.12.301

This paper follows a recent similar review [6] and summarizes what was recently achieved, through the application of integrated computer models, to improve the understanding of radiation damage in materials under fusion relevant conditions. These new developments are applied to the interpretation of irradiation and mechanical tests, electron microscope observations, and transmutation-driven chemical transformations occurring in materials in conditions similar to those of a fusion power plant. We focus on the multiscale aspect of the problem and describe a hierarchy of methods that together form an integrated approach to fusion materials modelling.

2. The structure and mobility of elementary defects

Microstructural evolution of materials is driven by the accumulation, migration and agglomeration of radiation-induced defects, as well as by their interaction with solute and impurity atoms in the material. Recent density functional theory (DFT) calculations have dramatically improved our understanding of the structure of *small* defects. Here by 'small' we presently mean defects that have most of their strain energy stored in a region extending no further than four or five lattice periods away from the core of a defect. The structure of these defects can be determined by performing DFT calculations for simulation cells containing several hundreds of atoms. We find that in ferromagnetic bcc iron a self-interstitial atom (SIA) defect adopts the <1 1 0>-type configuration, while in all the non-magnetic bcc transition metals, including vanadium and tungsten, an interstitial defect has a linear one-dimensional <1 1 1> structure [7–10]. These two types of SIA defects are characterized by very different thermally activated mobilities. A <1 1 1> SIA easily glides through the lattice, and the temperatures of the resistivity recovery stages associated with the migration of SIA defects in the non-magnetic bcc transition metals do not exceed 40 K [10]. On the other hand, a <1 1 0> SIA defect in Fe migrates via a sequence of rotation-translation jumps [9], each time overcoming a potential barrier of ~0.34 eV. This gives rise to a resistivity recovery stage at ~107 K [11]. Vacancy formation and migration energies vary systematically following the Periodic Table [12], with migration energies of single vacancies varying between 0.62 eV in vanadium, 0.91 eV in chromium and 1.78 eV in tungsten [13]. The calculated migration energy of a vacancy in iron is 0.67 eV [14], and is the second lowest in the entire group of bcc transition metals. The formation energy of a vacancy in bcc iron (1.95 eV [7] or 2.07 [9]) is *the* lowest one among all the bcc transition metals [15]. The even lower values of vacancy formation energies in the range between 1.59 and 1.73 eV reported in earlier experiments [16] were likely caused by the presence of carbon. Carbon forms bound complexes with vacancies, and the binding energy of a V–C complex is of the order of 0.4 eV [14]. This reduces the *visible* formation energy of a vacancy in carbon-contaminated iron (which is no longer the formation energy of a vacancy but rather the formation energy of a V–C complex) from approximately 2.0 eV down to 1.6 eV.

Both vacancies and SIA defects form clusters [14]. The driving force for clustering is strong in the case of SIA defects, where the energy of formation (per SIA) of a cluster decreases with every new SIA joining the cluster. For example, the energy of a di-interstitial cluster in iron is 0.8 eV lower than the energy of two separate SIA <1 1 0> dumbbells. In the macroscopic limit the amount of energy per SIA released through clustering asymptotically approaches the formation energy of an individual SIA defect, which in the case of iron is between 3.6 eV and 4 eV [7,9]. In tungsten the formation energy of an SIA defect exceeds 9.5 eV [10,15] and the driving force for clustering is very strong. Vacancies also form clusters, but the binding energy per vacancy in a vacancy cluster is lower [14]. Vacancy clusters dissociate and evaporate at elevated temperatures, while SIA clusters do not.

The treatment of interaction of SIA and vacancy defects with carbon, nitrogen and other impurity and/or solute atoms at elevated temperatures is one of the key objectives for modelling microstructural evolution of steels under irradiation. In ferromagnetic bcc iron, interstitial carbon and nitrogen atoms occupy the octahedral lattice sites [18]. Carbon and nitrogen migrate via the tetrahedrally-coordinated saddle points, and the activation energies for migration are high, ~0.9 eV for carbon and ~0.75 eV for nitrogen [18]. Carbon forms strongly bound complexes with vacancies. These complexes are thermally fairly stable since their dissociation is impeded by the low mobility of the constituting vacancies and carbon atoms. Even if a vacancy-carbon complex dissociates in the lattice, the individual vacancy and the carbon atom have difficulty separating by thermally activated migration. The binding energy of a vacancy-carbon complex is 0.41 eV, and the migration energy of a vacancy is 0.67 eV (the energy of migration of a carbon atom is even higher), giving rise to the dissociation energy of a vacancy-carbon complex of 1.08 eV [14]. Similarly, the energy of binding of a nitrogen atom to a vacancy is 0.71 eV [18], and the dissociation energy for a vacancy-nitrogen complex is 1.38 eV. Interaction between an SIA defect and a carbon or a nitrogen atom is comparatively weak [18], and so far no strongly bound SIA-C or SIA-N configuration has been found.

Chromium is the main alloying element in EUROFER steel. The striking fact, illustrated in Fig. 1, that the enthalpy of formation of a binary FeCr alloy changes sign at ~10% Cr concentration in the ferromagnetic state but *does not* change sign in the paramagnetic state was discovered by Olsson et al. [19,20] using *ab-initio* calculations. This finding illustrates the fundamental role played by the electron exchange and correlations effects, which give rise to spin polarization, in the phase stability of FeCr and other iron-based alloys.

Vacancies migrate much slower in chromium than in iron [13,21] (the energy of migration of a vacancy in chromium is 0.91 eV compared to 0.67 eV in iron), in striking agreement with observations [22] showing that the activation energy for self-diffusion in pure chromium is 3.51 ± 0.13 eV, compared with the predicted value of 3.55 eV [9,10,15] (the activation energy for self-diffusion is the sum of vacancy formation and migration energies). In FeCr alloys migration of vacancies is influenced by Cr atoms, with the maximum of the interdiffusion coefficient occurring at ~13% Cr [23]. Analysis of resistivity recovery curves [24] suggests that the presence of Cr atoms has a significant effect on the transport of SIA defects to sinks, which may be interpreted in terms of trapping and de-trapping of SIAs [25] as well as in terms of Cr-assisted diffusion of SIAs at low temperatures, or in terms of the

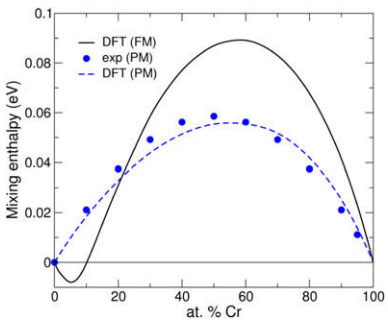

Fig. 1. The formation energy (the mixing enthalpy) of ferromagnetically (FM) and paramagnetically (PM) ordered binary FeCr alloys [19], [20]. The density functional calculations were performed using the Coherent Potential Approximation (CPA) in which the alloy is treated as a random mixture of Fe and Cr atoms [21].

confinement of SIAs by the solute atoms [26]. Although Cr atoms have a slightly larger size than Fe atoms, DFT calculations show that SIA defects form weakly bound states with individual Cr solute atoms. In ferromagnetic bcc iron, binding between an SIA and a Cr atom is unusually strong for the case of a <1 1 1> crowdion configuration of the SIA defect (which notably is not the lowest energy SIA configuration in bcc Fe), and the binding energy is of the order of 0.4 eV [27]. This result suggests that the mobility of small SIA clusters containing more than five self-interstitial atoms and resembling the *a/2*(1 1 1) prismatic glissile dislocation loops [17] may be affected by the interaction with Cr solute atoms [28]. Traps for migrating SIA defects in concentrated FeCr alloys may also be associated with clusters of Cr atoms.

3. Production and clustering of radiation defects

There is still only one viable way of modelling the fast non-equilibrium collision events (cascades) that produce defects under neutron or ion irradiation. Since atoms in a collision cascade are strongly displaced from their equilibrium positions in the lattice, to find the outcome of a cascade event and to predict how many defects are formed, and of what type, one has to investigate solutions of the classical equations of motion of atoms $m\frac{d^2\mathbf{R}_a}{dt^2} = -\frac{\partial}{\partial \mathbf{R}_a}U(\mathbf{R_1}, \mathbf{R}_2, ..., \mathbf{R}_N)$, where $U(\mathbf{R_1}, \mathbf{R}_2, ..., \mathbf{R}_N)$ is the potential energy for a set of positions of atoms $\mathbf{R_1}, \mathbf{R}_2, ..., \mathbf{R}_N$. Numerical integration of these differential equations for each atom a is a well defined mathematical procedure, and the choice of the functional representation of the potential energy (the "interatomic potential" $U(\mathbf{R_1}, \mathbf{R}_2, ..., \mathbf{R}_N)$) is the main factor determining the degree of realism of a simulation.

There is no unique or fully satisfactory scheme for deriving an interatomic potential. DFT is an approximation in its own right and, as a *variational* approach based on the minimization of a value of a certain postulated energy functional, it offers limited insight into *why* the total energy is minimum for a certain atomic configuration. Interatomic potentials are derived using various simplifications and assumptions: for example, the model tight-binding Hamiltonians [29]. These Hamiltonians often neglect terms representing electron-electron interaction, which in fact *are* included in DFT through the use of exchange-correlation functionals. For example, the bcc crystal structure of iron is stabilized by exchange-correlation effects, which give rise to ferromagnetism. In a model Hamiltonian exchange and correlation effects can be treated using the Hubbard and the Stoner terms [30,31]. However, so far only one semi-empirical potential has been derived that takes into account exchange interactions for a simple case of the Stoner Hamiltonian [32].

The bond-order potential (BOP) formalism [33,34] is a computational scheme for the evaluation of total energies and interatomic forces based on the tight-binding approximation and the concept of the *local* electronic structure. So far it has not been extensively applied to the simulation of radiation damage, and estimates show that a BOP-based MD treatment of magnetic materials may be a factor of 10, or more, slower than conventional semi-empirical potentials. This comparatively high (though still low if compared with DFT) computational cost comes from the need to evaluate contributions from hopping pathways involving many atoms, and also from a numerical self-consistency loop required for the iterative evaluation of magnetic moments, even in the mean-field approximation. Still, this approach may offer a way forward in the development of approximations since there is now direct evidence that exchange and correlation effects prevent segregation of Cr atoms in dilute FeCr alloys [20,35], are responsible for spin fluctuations driving the α–γ bcc–fcc phase transitions [36], and give rise to dislocation instabilities at elevated temperatures [37]. Hence the treatment of electronic structure linked to the derivation of semi-empirical potentials represents a natural and necessary step in the development of models for these effects.

Given the uncertainty of approximations underlying the choice of the functional form and the parameters describing the interaction between atoms in the semi-empirical potential formalism, several functions $U(\mathbf{R_1}, \mathbf{R}_2, ..., \mathbf{R}_N)$, all of them describing bcc iron, were proposed in recent years. A comparative test of three of such model potentials for pure bcc Fe was carried out in [38]. The results of the test are illustrated in Fig. 2. The test shows that the numbers of defects formed in collision cascades modelled using the three different potentials are in good agreement with each other. At the same time there are considerable fluctuations in the predicted clustering probabilities for both the SIAs and vacancies. These fluctuations likely reflect the differences in the binding energies between defects, as well as other features of the potentials [39]. For example, analysis performed in [15] showed that di-vacancy binding energies predicted by the semi-empirical potentials fluctuated by as much as ±0.1 eV in comparison with the DFT values. Cascade simulations performed for FeCr alloys show that the presence of Cr atoms *does not* have a significant effect on the generation of defects [40–42]. This, by no means obvious, conclusion agrees with simulations [43] performed independently using a different FeCr potential. Hence the systematic variation of the defect production efficiency and systematic changes in the microstructure of irradiated alloys observed as a function of Cr concentration [44] is likely associated not with the production of defects [45,46], but rather with the *relatively* long-term evolution of microstructure, i.e. with the effect of chromium atoms on the thermal mobility and diffusion, as well as on the rate of annihilation and agglomeration of radiation defects.

The mobility of defects in pure metals and in FeCr alloys were investigated using molecular dynamics (MD) simulations [25,28,45,46]. The temperature dependence of the diffusion of vacancies or the relatively immobile SIA defects (for example, individual <1 1 0> dumbbells or small clusters of SIAs in iron) follows the Arrhenius law $D(T) \sim D_0\ exp(-E_a/k_BT)$, where E_a is the activation energy for migration. At the same time the statistics of migration of small glissile interstitial dislocation loops is largely non-Arrhenius, and at elevated temperatures the diffusion coefficient of a nano-dislocation loop in a pure metal is expected to vary linearly as a function of temperature, $D(T) \sim T$ [47,15,48].

4. Multi-scale treatment of microstructural evolution

A striking evidence for the significant part played by multiscale effects in microstructural evolution of irradiated materials is provided by the recent *in-situ* experimental observations of migration of nano-dislocation loops in irradiated iron [49,44]. Experimental observations show that the diffusion coefficient of a small dislocation loop in iron is $\sim$50 nm^2/s, whereas MD simulations predict that loops diffuse approximately eight orders of magnitude faster. The rate-limiting stage for the diffusion of nano-dislocation loops in iron is their interaction with impurities, for example carbon or nitrogen, or carbon-vacancy, or nitrogen-vacancy complexes. This gives rise to the observed high activation energy for migration $\sim$1.3 eV, which is very close to the dissociation energy for a vacancy-nitrogen complex, and is two orders of magnitude higher than the activated energy for migration predicted by simulations for pure iron [45,48]. The fundamental difficulty associated with modelling the slow modes of evolution of defects associated with the pinning of migration defects by impurities, is that these modes of evolution form smooth envelopes for the rapidly fluctuating quantities, for example, the position of the centre of a nano-dislocation loop, illustrated in the left panel of Fig. 3. The fast

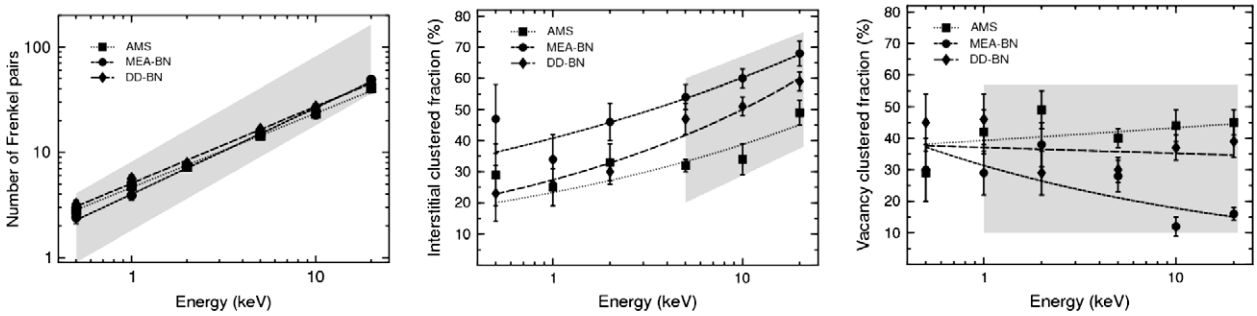

Fig. 2. Comparison of defect production rates predicted by collision cascade simulations performed using three different interatomic potentials [38].

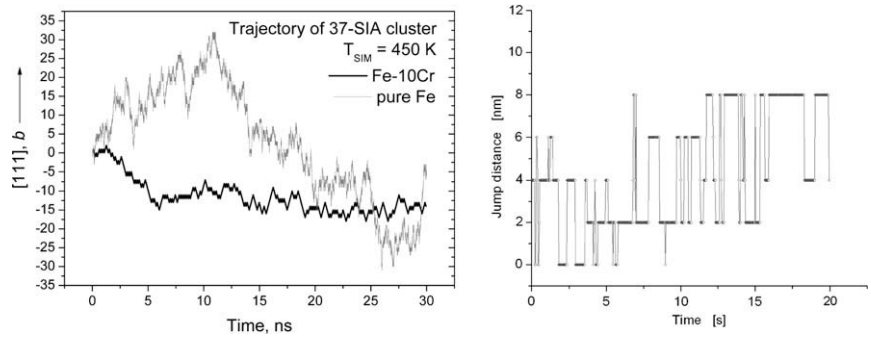

Fig. 3. Trajectories of migrating nano-dislocation loops simulated using MD for pure Fe and Fe-10%Cr alloy (left) and a trajectory of a loop migrating in nominally pure Fe at 300 °C observed experimentally (right). Note the nine orders of magnitude difference between the timescales of simulations and experimental observations, and the fact that the trajectory of migration of a loop in the FeCr alloy exhibits longer periods of residence of the migrating loop in the material. This correlates somewhat better with experimental observations showing that loops do not migrate continuously but rather 'hop' between spatially confined configurations.

fluctuating behaviour of dislocation loops found in molecular dynamics simulations is perfectly real. The velocity of a migrating loop derived from the equipartition principle $m^*V^2 \sim k_BT$ approaches hundreds of meters per second, and hops between pinning sites appear instantaneous on the timescale of experimental observations (~1/30th of a second). At the same time a pinning event, where a loop resides at a certain point for a second or longer (see the right panel of Fig. 3), cannot possibly be treated using MD. Kinetic Monte Carlo (kMC) and rate theory algorithms offer a way forward in bridging the gap between the nano-second timescale accessible to MD and the "human" timescale of seconds, weeks and years [50,51]. In this context we note the new significant development of a synchronous parallel kinetic Monte-Carlo model for continuum diffusion-reaction systems and its first applications described in Ref. [52].

The mobility of dislocations in bcc metals is also characterized by well defined activation energies. Experimental studies of the ductile-brittle transition in bcc transition metals show that the effective activation energies characterizing the transition vary between E_a = 0.26 eV in pure highly annealed vanadium, E_a = 0.33 eV in crystalline iron, E_a = 0.49 eV in molybdenum, and E_a = 1.05 eV in pure crystalline tungsten [53]. Fig. 4 illustrates the linear relation between the inverted ductile-brittle transition temperature (DBTT) and the logarithm of the critical strain rate *at* the DBTT. The activation energies for DBTT are close to one half of the formation energy E_{DK} for a double kink on a <1 1 1> screw dislocation (in tungsten E_{DK} ~2.05 eV, in molybdenum E_{DK} ~1.2 eV and in iron E_{DK} ~0.7 eV) in agreement with the double-kink model for the mobility of a screw dislocation [55]. This confirms the dislocation mobility-based concept of the ductile-brittle transition [56], and the pivotal role played by the screw rather than edge dislocations in the plasticity of bcc metals. We note that the measured value of the activation energy for DBTT in crystalline vanadium E_a = 0.26 eV [54] suggests that in this metal the energy of formation of a double kink on a <1 1 1> screw dislocation is E_{DK} ~0.55 eV.

The interpretation of experimental data on DBTT is based on the treatment of self-organized dislocation ensembles in the plastic zone [57]. In this treatment the mobility of dislocations is controlled by the effective activation energy $E_a = E_{DK} - V\cdot\tau$, where V is the activation volume for the formation of a double kink and τ is the net self-consistent shear stress acting on the dislocations. The fact that the activation energy for migration of screw dislocations in various metals can be systematically determined by investigating the strain dependence of the DBTT [53] as well as the fact, illustrated in Fig. 4, that the activation energy for migration of dislocations in sintered tungsten is visibly greater than that in pure single crystalline tungsten suggests that an experimental investigation of dislocation mobility in irradiated materials may provide quantitative information about the nature of microscopic interactions between dislocations and precipitates, and radiation-induced defects.

It may also be possible to characterize the part played by thermal activation in the picture of deformation of a composite material, for example oxide-dispersion strengthened (ODS) steel [58]. The dislocation mobility laws enter the equations for discrete dislocation dynamics (DDD) simulations as parameters of differential equations describing the dynamics of the system, which is in some way similar to how interatomic potentials enter the MD equations. The availability of accurately parameterized dislocation mobility laws for bcc transition metals is a necessary requirement for a realistic simulation of plastic behaviour of fusion materials. The primary issue here is a realistic description of the mobility of screw dislocations as a function of applied stress *and* temperature. Another challenge for a DDD model is the parameterization of the pencil glide, which is a sequence of cross-slip events. A DDD model must also describe reactions between dislocations in a bcc metal.

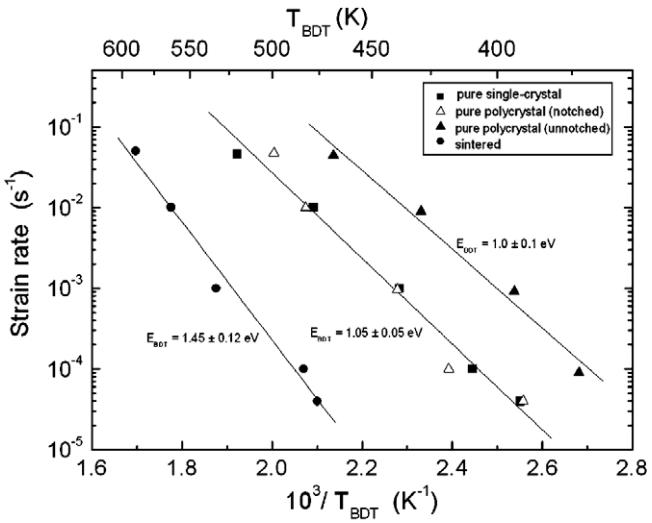

Fig. 4. Arrhenius-law fits showing a correlation between the temperature of the brittle-ductile transition in tungsten, and the strain rate at which the transition occurs [53,54].

For instance, a reaction between two <1 1 1> dislocations may lead to a formation of a dislocation with a <1 0 0> Burgers vector. Even though the formation of such dislocations is geometrically possible, it is not known *a priori* to what extent they may influence the movement of the original dislocations.

Can MD simulations help with parameterizing dislocation mobility laws? We noted above that the observed values of activation energy for mobility of dislocations in bcc metals are correlated with the formation energy E_{DK} of a double kink on a <1 1 1> screw dislocation. In the case of iron the predicted values of E_{DK} vary between 0.4 eV for the Simonelli potential [59], 1.1 eV for the magnetic potential [60], and ~1.7 eV for the Mendelev potential [59], compared to the experimental value of E_{DK} ~0.7 eV. The most recent calculations [61,62] performed for the Mendelev potential predict the double kink formation energies that are in better agreement with experiment, namely E_{DK} ~0.65 eV [61] or E_{DK} ~0.75 eV [62].

While describing plastic deformations only in the limit of high strain rates, MD simulations provide valuable insights into the nature of microscopic interactions between mobile dislocations and radiation defects. For example, the effect of temperature and the strain rate on the interaction of an edge dislocation with SIA clusters was investigated in [63]. It was found that temperature plays a significant part effectively deciding the outcome of a simulation. Simulations performed at low temperatures show that a moving dislocation line experiences strong resistance when encountering an SIA cluster, while the high temperature simulations show the partial dissolution of an SIA cluster (a nano-dislocation loop) by a moving dislocation. The significant part played by the screw component of a dislocation line was illustrated by a recent MD study of interaction between an edge dislocation and a cavity [64] where it was found that the obstacle strength was largely determined by the length of the screw segment formed just before the release of the dislocation from the obstacle.

Concluding this section, we note a new approach to the treatment of dislocation mobility based on DFT calculations. These calculations require using simulation cells containing many more atoms than those used for the investigation of point defects, and hence it is natural to start from the investigation of a perfect linear dislocation configuration. The structure of the core of a <1 1 1> screw dislocation and the Peierls barrier for the translational two-dimensional motion of this dislocation (not involving the double kink mechanism) was studied in [65]. *Ab-initio* calculations make it possible to select an interatomic potential (in the case studied in [65] it was found to be the potential developed in [66]) that agrees best with the DFT data.

5. Phase stability and dynamics on the "human" timescale

One of the significant problems associated with the development of materials for fusion technology is the expected change in the chemical composition of a material, and the generation of transmutation elements, in the first place helium, by the inelastic nuclear collisions initiated by the fusion neutrons, see e.g. Table 1 of Ref. [67]. At the end of a 5 year period of operation of a fusion power plant the steel used in the first wall is expected to contain approximately 0.15 atomic percent of helium. Helium atoms formed by transmutation rapidly diffuse through the lattice and fill the vacant lattice sites, creating substitutional He atoms, which can also be treated as He–V binary complexes. The calculated binding energy of a He–V complex is 2.3 eV [68]. This He–V complex grows by absorbing migrating helium atoms and vacancies, resulting in the formation of a small and fairly stable mesoscopic helium-vacancy cluster. A quantitative kinetic Monte Carlo model for the growth of a small helium-vacancy cluster based on *ab-initio* calculations of energy barriers for the attachment/detachment of individual vacancies and helium atoms is described in Ref. [68]. Simulations described in Ref. [68] suggest that impurities have a significant effect on the evolution of helium clusters and on the rate of desorption of He from the material. For example, the effective energy for migration of a vacancy had to be increased from 0.67 eV to 0.83 eV and the binding energies of He–V and He–V_2 clusters had to be reduced from 2.3 eV and 0.78 eV to 1.78 eV and 0.54 eV respectively to match the experimentally observed He desorption curves. The SIA clusters had to be assumed to be immobile, in agreement with experimental observations [49] showing the high activation energies for migration of the clusters due to the trapping effect of impurities in the material [67].

Ab-initio calculations of energies of various He defect configurations given in [69–71] showed that the energy of solution of a helium atom in iron (4.39 eV) exceeds the formation energy of an SIA. Hence clustering of interstitial helium atoms can give rise to the spontaneous formation ('emission') of SIA defects. Fig. 5 shows that a cluster containing three helium atoms in principle can grow (by attracting another interstitial helium atom from the surrounding lattice) via the emission of an SIA. This process is equivalent to the spontaneous creation of a Frenkel pair with the vacancy immediately absorbed by the helium cluster.

In addition to absorbing freely migrating vacancies and forming bubbles, helium atoms segregate to the parts of microstructure (e.g. grain boundaries) characterized by the excess of free volume [72]. *Ab-initio* methods have now been applied to the investigation of segregation and migration of He near grain boundaries [73].

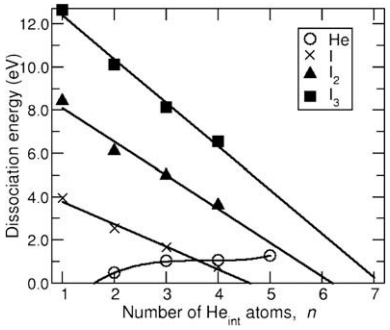

Fig. 5. Dissociation energies of a He atom, a mono-, di-, or tri-interstitials from a small interstitial He_n cluster [70].

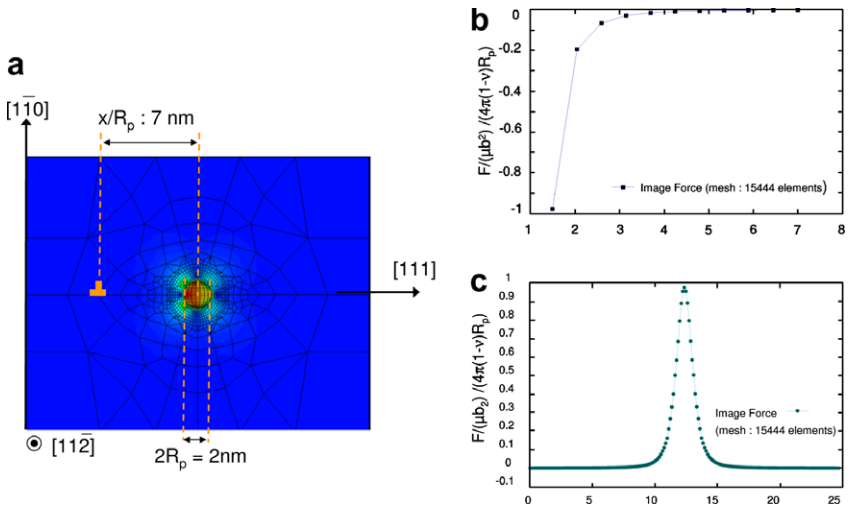

Fig. 6. (Left) Mesh used in the treatment of a He bubble-dislocation interaction in a DDD-FE code; (Bottom right) The image force (normalized) along the dislocation and (top right) the image force (normalized) as a function of the distance to the cavity.

The presence of helium clusters in a material contributes to radiation hardening. This was investigated in [74], where it was found that helium clusters (bubbles) do not give rise to substantial hardening, whereas the self-interstitial dislocation loops emitted by helium bubbles do represent strong obstacles for the propagation of dislocations. Only the helium bubbles characterized by high helium per vacancy ratio and hence approaching the threshold for the spontaneous emission of SIA loops are able to significantly impede the propagation of dislocations [64]. Simulations of cascades carried out assuming randomly distributed helium atoms did not show a significant effect of helium on the Frenkel pair production [75]. In principle, one might expect that the formation of helium clusters in cascades would stimulate the production of SIA defects through the emission mechanism illustrated in Fig. 5. However, the operation of this mechanism depends on the fine balance between the energy of formation of an SIA and the energy gained through clustering of helium atoms and vacancies, as well as on the assumed initial distribution of helium atoms in the matrix. This balance depends on the choice of an interatomic potential used in a simulation. An MD study of helium cluster formation in collision cascades in tungsten [76] showed that the formation of helium clusters was indeed accompanied by punching of SIA dislocation loops.

To investigate the hardening effect of helium bubbles on the mesoscale, Discrete Dislocation Dynamics (DDD) simulations were performed to verify whether the local reaction rules identified in MD simulations for a dislocation interacting with a He bubble are mainly associated with the dislocation core effects, or if the elasticity-based treatment already provides a reasonably accurate approximation. A DDD code coupled to a Finite Elements Method (FEM) code was applied to describe the image forces induced by the cavity. Local rules for the dislocation-bubbles interaction have been derived, and presently are being implemented for the future use in large scale dislocation dynamics simulations, as illustrated in Fig. 6.

A particularly significant composition-related aspect of the phase stability of steels under irradiation is associated with the segregation of Cr atoms. We have already noted the magnetic anomaly of the phase diagram occurring in the FeCr alloys in the limit of low Cr concentration. Several approximate schemes have been proposed recently to extend these results to larger system sizes and to longer timescales. These new results involve the development of semi-empirical interatomic potentials and application of those to MD and kMC simulations [77–80], as well as to the development of the cluster expansion formalism, where interaction between atoms *on a bcc lattice* is described by a small set of coefficients derived directly from DFT calculations [81]. Both approaches claim partial successes in modelling the temperature-concentration phase diagram, although none has so far been applied to the treatment of the fcc γ-loop and the σ-phase. The *magnetic* cluster expansion [82] is now able to model both the configurational *and* orientational magnetic disorder in FeCr alloys, potentially offering a way of explaining the observed correlation between the magnetic properties of EUROFER and the loss of tensile strength of steel at elevated temperatures [83,84].

6. Conclusions and outlook

This review describes the result of a recent substantial effort focused on understanding the fundamentals of radiation damage in fusion materials, and on the development of quantitative mathematical models for the observed effects. The complexity of the problem is difficult to overstate, and the issues that one faces here require using the most advanced available mathematical concepts and simulation techniques. The EU fusion materials modelling programme has succeeded in bringing together a diverse group of experts in materials modelling whose work already addressed many issues of practical significance, and has developed close links with experimental work. We expect that the commissioning of new materials testing facilities, especially accelerator facilities for multiple ion beam irradiation [85], and further extensive interaction with experimental groups will enhance the future role played by mathematical modelling in the fusion materials and technology programmes.

Acknowledgements

The authors gratefully acknowledge discussions with M. Victoria, G. Martin, and B.N. Singh, who established the EU fusion materials programme. The authors would like to thank P. Olsson, C. Björkas, Z. Yao, M.L. Jenkins, S.G. Roberts and E. Ferrié, who kindly provided graphical material used in this paper.

References

[1] E.P. Wigner, Commun. Pure Appl. Math. 13 (1960) 1.
[2] R.A. Jameson, R. Ferdinand, H. Klein, J. Rathke, J. Sredniawski, M. Sugimoto, J. Nucl. Mater. 329–333 (2004) 193.
[3] P. Jung, J. Henry, J. Chen, J.-C. Brachet, J. Nucl. Mater. 318 (2003) 241.

[4] J. Henry, M.-H. Mathon, P. Jung, J. Nucl. Mater. 318 (2003) 249.
[5] M.H. Mathon, Y. de Carlan, G. Geoffroy, X. Averty, A. Alamo, C.H. de Novion, J. Nucl. Mater. 312 (2003) 236.
[6] M. Victoria, S.L. Dudarev, J.-L. Boutard, E. Diegele, R. Lässer, A. Almazouzi, M.-J. Caturla, C.-C. Fu, J. Källne, L. Malerba, K. Nordlund, M. Perlado, M. Rieth, M. Samaras, R. Schäublin, B.N. Singh, F. Willaime, Fus. Eng. Des. 82 (2007) 2413.
[7] C. Domain, C.S. Becquart, Phys. Rev. B65 (2001) 024103.
[8] S. Han, L.A. Zepeda-Ruiz, G.J. Ackland, R. Car, D.J. Srolovitz, Phys. Rev. B66 (2002) 220101.
[9] C.C. Fu, F. Willaime, P. Ordejón, Phys. Rev. Lett. 92 (2004) 175503.
[10] D. Nguyen-Manh, A.P. Horsfield, S.L. Dudarev, Phys. Rev. B73 (2006) 020101; S.P. Fitzgerald, D. Nguyen-Manh, Phys. Rev. Lett. 101 (2008) 115504.
[11] C.C. Fu, J. Dalla Torre, F. Willaime, J.-L. Bocquet, A. Barbu, Nat. Mater. 4 (2005) 68.
[12] F. Willaime, A. Satta, M. Nastar, O. Le Bacq, Intern. Journ. Quant. Chem. 77 (2000) 927.
[13] D. Nguyen-Manh, S.L. Dudarev, A.P. Horsfield, J. Nucl. Mater. 367–370 (2007) 257.
[14] C.-C. Fu, F. Willaime, Comptes Rendus Physique 9 (2008) 335.
[15] P.M. Derlet, D. Nguyen-Manh, S.L. Dudarev, Phys. Rev. B76 (2007) 054107.
[16] K. Fürderer, K.-P. Döring, M. Gladisch, et al., Mater. Sci. Forum 15–18 (1987) 125.
[17] F. Willaime, C.-C. Fu, M.C. Marinica, J. Dalla Torre, Nucl. Instr. Meth. Phys. Res. B228 (2005) 92.
[18] C. Domain, C.S. Becquart, J. Foct. Phys. Rev. B69 (2004) 144112; D. Nguyen-Manh, Adv. Mater. Res. 59 (2009) 253.
[19] P. Olsson (2002) private communication.; P. Olsson, I.A. Abrikosov, J. Wallenius, Phys. Rev. B73 (2006) 104416.
[20] P. Olsson, I.A. Abrikosov, L. Vitos, J. Wallenius, J. Nucl. Mater. 321 (2003) 84.
[21] D. Nguyen-Manh, M.Y. Lavrentiev, S.L. Dudarev, Comptes Rendus Physique 9 (2008) 379.
[22] J.L. Campbell, C.W. Schlute, Appl. Phys. A19 (1979) 149.
[23] R. Braun, M. Feller-Kniepmeier, Phys. Stat. Sol. A90 (1985) 553.
[24] A.L. Nikolaev, Philos. Mag. 87 (2007) 4847.
[25] D. Terentyev, P. Olsson, T.P.C. Klaver, L. Malerba, Computational Materials Science 43 (2008) 1183.
[26] T.S. Hudson, S.L. Dudarev, A.P. Sutton, Proc. Roy. Soc. London A460 (2004) 2457.
[27] P. Olsson, C. Domain, J. Wallenius, Phys. Rev. B75 (2007) 014110.
[28] D.A. Terentyev, P. Olsson, L. Malerba, A.V. Barashev, J. Nucl. Mater. 362 (2007) 167.
[29] Modelling Electrons and Atoms for Materials Science. in: Proceedings of D.G. Pettifor's 60th Birthday Celebration Symposium, M.W. Finnis, R. Drautz (Eds.), Prog. Mater. Sci. 52 (2007) 131–463.
[30] S.L. Dudarev, P.M. Derlet, J. Comput. Aided Mater. Des. 14 (Suppl. 1) (2007) 129.
[31] G. Liu, D. Nguyen-Manh, B.G. Liu, D.G. Pettifor, Phys. Rev. B71 (2005) 174115.
[32] S.L. Dudarev, P.M. Derlet, J. Phys. Cond. Matt. 17 (2005) 7097; P.M. Derlet, S.L. Dudarev, Prog. Mater. Sci. 52 (2007) 299.
[33] R. Drautz, D.G. Pettifor, Phys. Rev. B74 (2006) 174117.
[34] M. Mrovec, D. Nguyen-Manh, C. Elsasser, P. Gumbsch, D.G. Pettifor, in: Proceedings of Materials Research Society 2007 Fall Meeting, Boston, 26–30 November 2007.
[35] T.P.C. Klaver, R. Drautz, M.W. Finnis, Phys. Rev. B74 (2006) 094435.
[36] H. Hasegawa, M.W. Finnis, D.G. Pettifor, J. Phys. F: Metal Phy. 15 (1985) 19.
[37] S.L. Dudarev, R. Bullough, P.M. Derlet, Phys. Rev. Lett. 100 (2008) 135503; S.L. Dudarev, P.M. Derlet, R. Bullough, J. Nucl. Mater. 386–388 (2009) 45.
[38] C. Björkas, K. Nordlund, Nucl. Instr. Meth. B259 (2007) 853.
[39] L. Malerba, J. Nucl. Mater. 351 (2006) 28.
[40] N. Juslin, K. Nordlund, J. Wallenius, L. Malerba, Nucl. Instr. Meth. B255 (2007) 75.
[41] D.A. Terentyev, L. Malerba, R. Chakarova, K. Nordlund, P. Olsson, M. Rieth, J. Wallenius, J. Nucl. Mater. 349 (2006) 119.
[42] C. Björkas, K. Nordlund, L. Malerba, D. Terentyev, P. Olsson, J. Nucl. Mater. 372 (2008) 312.
[43] J.-H. Shim, H.-J. Lee, B.D. Wirth, J. Nucl. Mater. 351 (2006) 56.
[44] Z. Yao, M. Hernandez-Mayoral, M.L. Jenkins, M.A. Kirk, Philos. Mag. 88 (2008) 2851, 2881.
[45] D.A. Terentyev, L. Malerba, M. Hou, Phys. Rev. B75 (2007) 104108.
[46] L. Malerba, D.A. Terentyev, G. Bonny, A.V. Barashev, C. Björkas, N. Juslin, K. Nordlund, C. Domain, P. Olsson, N. Sandberg, J. Wallenius, J. ASTM Intern. 4 (2007) 1.
[47] L.A. Zepeda-Ruiz, J. Rottler, S. Han, G.J. Ackland, R. Car, D.J. Srolovitz, Phys. Rev. B70 (2004) 060102; L.A. Zepeda-Ruiz, J. Rottler, B.D. Wirth, R. Car, D.J. Srolovitz, Acta Materialia 53 (2005) 1985.
[48] S.L. Dudarev, Comptes Rendus Physique 9 (2008) 409.
[49] K. Arakawa, K. Ono, M. Isshiki, K. Mimura, M. Uchikoshi, H. Mori, Science 318 (2007) 956.
[50] C.J. Ortiz, M.J. Caturla, Phys. Rev. B75 (2007) 184101.
[51] C.J. Ortiz, M.J. Caturla, C.C. Fu, F. Willaime, Phys. Rev. B75 (2007) 100102.
[52] E. Martinez, J. Marian, M.H. Kalos, J.M. Perlado, J. Comput. Phys. 227 (2008) 3804.
[53] A. Giannatasio, M. Tanaka, T.D. Joseph, S.G. Roberts, Physica Scripta T128 (2006) 87.
[54] T.D. Joseph, M. Tanaka, A.J. Wilkinson, S.G. Roberts, J. Nucl. Mater. 367–370 (2007) 637.
[55] J.P. Hirth, J. Lothe, Theory of Dislocations, Krieger, Florida, 1992. p. 545.
[56] P.B. Hirsch, S.G. Roberts, J. Samuele, Proc. Roy. Soc. London A421 (1989) 25.
[57] M. Tanaka, E. Tarleton, S.G. Roberts, Acta Materialia 56 (2008) 5123.
[58] B. Bako, D. Weygand, M. Samaras, J. Chen, M.A. Pouchon, P. Gumbsch, W. Hoffelner, Philos. Mag. 87 (2007) 3645.
[59] J. Chaussidon, M. Fivel, D. Rodney, Acta Mater. 54 (2006) 3407.
[60] P.M. Derlet, 2006, M.R. Gilbert, 2007, private communications.
[61] L. Ventelon, F. Willaime, P. Leyronnas, J. Nucl. Mater. 386–388 (2009) 26.
[62] D. Terentyev, L. Malerba, Comput. Mater. Sci. 43 (2008) 855.
[63] D. Terentyev, L. Malerba, D.J. Bacon, Yu.N. Osetsky, Journ. Phys. Cond. Matt. 19 (2007) 456211.
[64] R. Schäublin, N. Baluc, Nucl. Fus. 47 (2007) 1690.
[65] L. Ventelon, F. Willaime, J. Comput. Aided Mater. Design 14 (Suppl. 1) (2007) 85.
[66] G.J. Ackland, M.I. Mendelev, D.J. Srolovitz, S. Han, A.V. Barashev, J. Phys.: Cond. Matter. 16 (2004) S2629.
[67] G.A. Cottrell, S.L. Dudarev, R.A. Forrest, J. Nucl. Mater. 325 (2004) 195.
[68] M.J. Caturla, C.J. Ortiz, C.-C. Fu, Comptes Rendus Physique 9 (2008) 401.
[69] C.-C. Fu, F. Willaime, Phys. Rev. B72 (2005) 064117.
[70] C.-C. Fu, F. Willaime, J. Nucl. Mater. 367–370 (2007) 244.
[71] T. Seletskaia, Y. Osetsky, R.E. Stoller, G.M. Stocks, Phys. Rev. Lett. 94 (2005) 046403.
[72] F. Gao, H. Heinisch, R.J. Kurtz, Journ. Nucl. Mater. 351 (2006) 133.
[73] C.-C. Fu, R. Soulairol, 2008, in preparation.
[74] R. Schäublin, Y.L. Chiu, J. Nucl. Mater. 362 (2007) 152.
[75] J. Yu, G. Yu, Z. Yao, R. Schäublin, J. Nucl. Mater. 367–370 (2007) 462.
[76] K.O.E. Henriksson, K. Nordlund, J. Keinonen, Nucl. Inst. Meth. B244 (2005) 377.
[77] J. Wallenius, P. Olsson, C. Lagerstedt, N. Sandberg, R. Chakarova, V. Pontikis, Phys. Rev. B69 (2004) 094103.
[78] J. Wallenius, P. Olsson, L. Malerba, D. Terentyev, Nucl. Instr. Meth. B255 (2007) 68.
[79] G. Bonny, D. Terentyev, L. Malerba, Comput. Mater. Sci. 42 (2008) 107.
[80] A. Caro, M. Caro, E.M. Lopasso, D.A. Crowson, Appl. Phys. Lett. 89 (2006) 121902.
[81] M.Y. Lavrentiev, R. Drautz, D. Nguyen-Manh, T.P.C. Klaver, S.L. Dudarev, Phys. Rev. B75 (2007) 014208.
[82] M.Y. Lavrentiev, S.L. Dudarev, D. Nguyen-Manh, J. Nucl. Mater. 386–388 (2009) 22.
[83] K. Mergia, N. Boukos, Journ. Nucl. Mater. 373 (2008) 1.
[84] S.P. Fitzgerald, S.L. Dudarev, Proceedings of the Royal Society London A464 (2008) 2549; S.P. Fitzgerald, S.L. Dudarev, Journ. Nucl. Mater. 386–388 (2009) 67.
[85] Y. Serruys, M.-O. Ruault, P. Trocellier, et al., Comptes Rendus Physique 9 (2008) 437.